Proposal of an All-Optical Flip-Flop Using a Cross-Coupled MMI Bistable Laser Diode

Mitsuru Takenaka and Yoshiaki Nakano
Research Center for Advanced Science and Technology, University of Tokyo, JST-CREST
7-3-1 Hongo, Bunkyo-ku, Tokyo, 113-8656, Japan
takenaka@hotaka.t.u-tokyo.ac.jp

We propose a novel bistable laser diode (BLD) with active multi-mode interference (MMI) cavity. Using FD-BPM, we predict that the MMI-BLD shows bistable switching between two cross-coupled modes, which can be utilized as an all-optical flip-flop or an optical memory.

Keywords: bistable laser diode, MMI coupler, two-mode bistability, all-optical flip-flop, FD-BPM

Introduction

Bistable laser diodes (BLDs) are expected to be important elements of future optical communications such as packet buffering, bit-length conversion, retiming, reshaping, demultiplexing, and wavelength conversion. However, conventional absorptive BLDs [1] have the difficulty of optical reset. To overcome this problem, two-mode intensity bistability [2], which originate from cross gain saturation between the two lasing modes, have been investigated. Although this type of bistability has been demonstrated by cross-coupled bistable laser diodes (XCBLDs) [3], they had a bit complicated waveguide structures.

In this paper, we propose a novel two-mode BLD including an active multi-mode interference (MMI) cavity (Fig.1). An all-optical flip-flop will be realized by the MMI-BLD whose simple structure is matched to the conventional LD fabrication technique. Moreover, it gets the benefits of the MMI's features, i.e, compactness, high design tolerances, a large optical bandwidth and polarization insensitivity. We design a 2 × 2 MMI which couples light signal from an input port totally into a cross output port. Two-mode bistability between two cross-coupled modes will occur in this configuration due to cross gain saturation. The static characteristics of the MMI-BLD are investigated using a finite difference beam propagation method (FD-BPM).

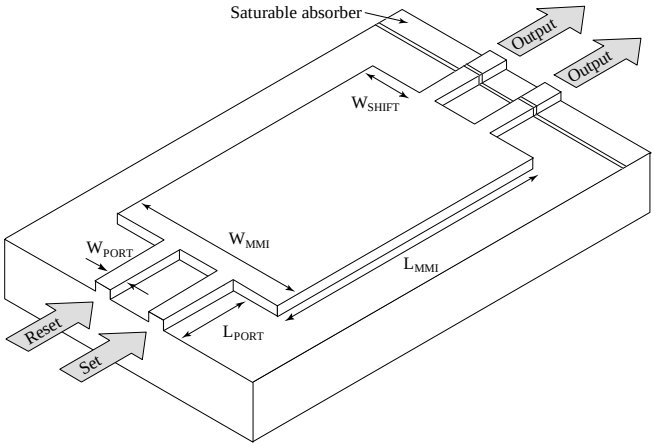

Fig. 1 Schematic view of MMI-BLD.

Simulation Method

The modeling of an MMI coupler requires special attention because several modes inside the coupler interfere with each other. Moreoever, the behavior of an active MMI coupler has been not well know yet. Therefore, we chose FD-BPM [4] which can treat complex distributions of photon, refractive index, and gain inside the cavity. However, the BPM models only take forward propagating lights into account, thus reflections inside the cavity are neglected. In this paper, we analyse uni-directionally forward and backward propagating lights, respectively, and only reflections from the cleaved facets of LDs [5] are considered.

In describing light propagation through the waveguides, the wave equation for a TE mode derived from Maxwell's equations is solved. The scalar Helmholtz equation for a TE-polarized light propagating a planar waveguide in the direction of *z* axis becomes:

$$\frac{\partial^2 E}{\partial z^2}+\frac{\partial^2 E}{\partial x^2}+k_0^2 n^2 E=0 \tag{1}$$

where $E(x, z)$ is the space-dependent electric field, $n(x, z)$ the space-dependent refractive index, k_0 the wave vector in vacuum and a temporal dependence of $\exp(j\omega t)$ is assumed. This equation can be reduced to the paraxial wave equation:

$$E(x,z)=\phi(x,z)\exp(-j\beta_0 z) \tag{2}$$

$$2j\beta_0\frac{\partial\phi}{\partial z}=\frac{\partial^2\phi}{\partial x^2}+(k_0^2 n^2-\beta_0^2)\phi \tag{3}$$

where β_0 is a reference propagation constant. Equation (3) is obtained by a slowly varying envelope approximation. It is solved using finite differences in the transverse (x) direction and a Cranck-Nicolson scheme for the longitudinal (z) coordinate. In order to avoid nonphysical reflections from the computational window edges, Hadley's transparent boundary condition [6] is implemented.

We also take photon-carrier interactions into account. To evaluate the carrier density $N(x, z)$, the steady-state carrier rate equation is expressed as:

$$\frac{J}{ed}=R(N)+\Gamma v_g g_1 S_1+\Gamma v_g g_2 S_2 \tag{4}$$

where J is the current density, e the electron charge, d the thickness of the active layer, R the recombination rate, Γ the confinement factor, v_g the group velocity, g the material gain and S the photon density (the subscripts 1 and 2 refer to the two cross-coupled modes in the MMI cavity respectively).

Using a detailed model including Auger recombination [7], the recombination rate is written as:

$$R(N)=c_1 N+c_2 N^2+c_3 N^3 \tag{5}$$

where c_1, c_2, and c_3 are recombination constants.

For the unsaturated material gain g_0, a linear dependence on carrier density is assumed:

$$g_0(N)=a(N-N_0) \tag{6}$$

where a is gain constants, N_0 the carrier density at transparency.

As two-mode bistability originates in cross gain saturation, it is necessary that this effect is included in bistability analysis. The saturated gains for the cross-coupled modes are related to the unsaturated gain g_0 through the photon densities of the two modes as follows:

$$g_1(N)=\frac{g_0}{1+\varepsilon_{11}S_1+\varepsilon_{12}S_2},\ g_2(N)=\frac{g_0}{1+\varepsilon_{22}S_2+\varepsilon_{21}S_1} \tag{7}$$

where ε_{11}, ε_{22} and ε_{12}, ε_{21} are the self-saturation and the cross-saturation coefficients, respectively.

To take into account the refractive index dependence on carrier density, a linearly dependent equation is assumed:

$$n=n_0+\frac{dn}{dN}N \tag{8}$$

where n_0 is the refractive index without carrier injection, and dn/dN is refractive index shift coefficient, which is taken to be negative. We only consider the refractive index change of the waveguide's core, whereas the refractive index of the clad is assumed to be fixed.

Bistability Analysis

An InGaAsP multiple quantum well (MQW) structure whose band gap energy is around 1.55 μm is studied. We assume that the self-saturation coefficient is 8.0×10^{-17} cm^3 and the cross-saturation coefficient is 1.6×10^{-16} cm^3. The other parameters are shown in [8].

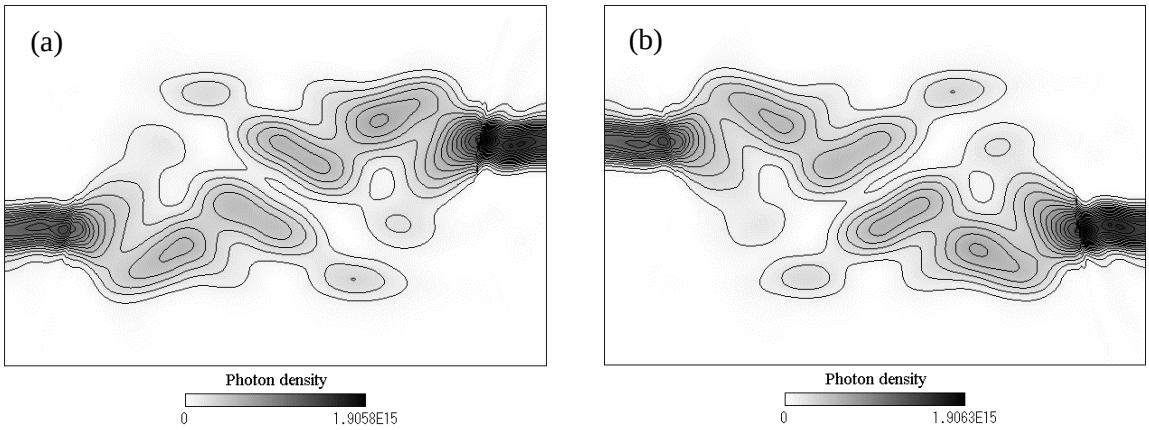

Fig. 2 Photon density [cm^{-3}] distributions of the MMI-BLD at (a) mode-1 and (b) mode-2.

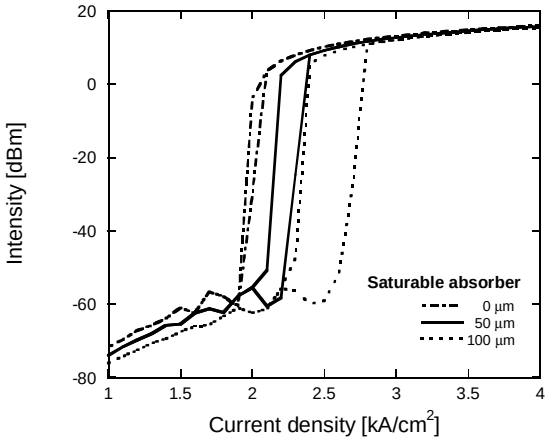

Fig. 3 L-I characteristics of the MMI-BLD with saturable absorber, 0, 50, and 100 μm.

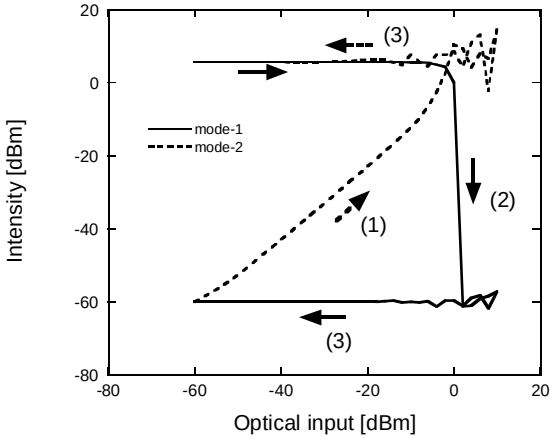

Fig. 4 Bistable switching characteristics of the MMI-BLD.

The 2 × 2 MMI coupler section should be designed in such a way that the input light totally couples into the cross output port. In the case of ridge waveguides whose refractive indices of core and clad are 3.255 and 3.24, respectively, the cross-coupled MMI coupler assumes the following physical dimensions: W_{MMI} = 12 μm, L_{MMI} = 540 μm, and W_{SHIFT} = 2.7 μm. The port width W_{PORT} and length L_{PORT} are 2 μm and 100 μm, respectively. In this design, the MMI-BLD has two cross-coupled lasing modes as shown in Fig. 2.

The saturable absorbers are equipped at the end of the output ports. Figure 3 shows L-I characteristics with the lengths of the saturable absorber (biased at 0.1 kA/cm^2) being 0, 50, and 100 μm, respectively. By increasing the saturable absorber length, the lasing threshold and the width of the hysteresis loop increase due to nonlinear absorption. The injection current of the gain region should be within the hysteresis loop in order to make use of the two-mode bistability. We adopt 50 μm as the saturable absorber length and 2.1 kA/cm^2 as the bias current density of the gain region.

External light injection of a set-signal saturates the absorption to mode-1, causing mode-1 to start lasing (ON state). At the same time cross gain saturation and the absorption to mode-2 by the saturable absorber suppress mode-2. In a similar manner, light injection of a reset-signal at the ON state suppresses mode-1 through cross gain saturation, therefore stopping laser oscillation in mode-1. Simultaneously, the absorption of mode-2's saturable absorber is decreased by the light injection to mode-2, resulting in lasing of mode-2 (OFF state). Even when the light injection is terminated, cross gain saturation and recovered absorption of the mode-1's absorber prevent mode-1 from

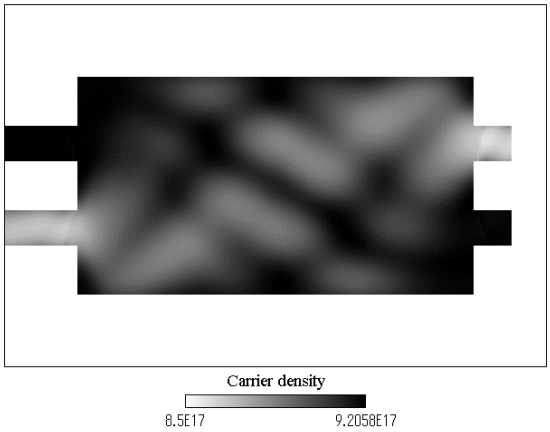

Fig. 5 Carrier density [cm^{-3}] distribution of the MMI-BLD lasing at mode-1.

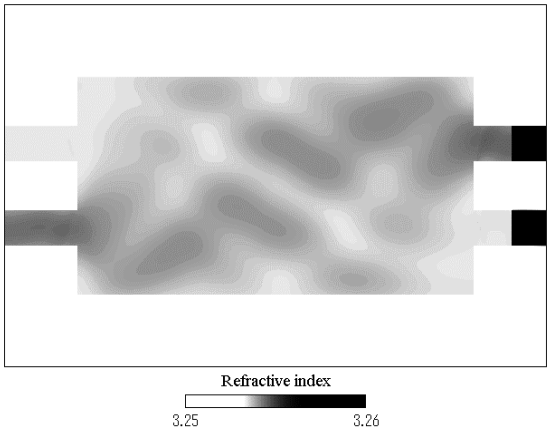

Fig. 6 Refractive index distribution of the MMI-BLD lasing at mode-1.

lasing again. Figure 4 shows this bistable switching characteristics. The MMI-BLD is set to the ON state by set-pulse at the beginning of the calculation. Increasing the optical injection to mode-2 (1) suddenly results in extinction of mode-1 (2) at around 0 dBm, thus switching MMI-BLD into the OFF state. When the optical injection is eliminated, the OFF state is maintained (3). As shown in Fig. 4, the two-mode bistability overcomes the optical reset problem of the absorptive BLDs, and the all-optical flip-flop operation will be realized using the MMI-BLD.

Figure 5 and 6 show the distributions of carrier density and refractive index in the case of the ON state, respectively. Because there were strong stimulated emission at the large optical intensity regions, the carrier distribution becomes uneven, i.e., spatial hole-burning occurs. Inside the MMI coupler, the range of the carrier density is 8.8×10^{17} to 9.2×10^{17} cm^{-3}. This difference of carrier density leads to the uneven distribution of refractive index, 3.2535 to 3.254 inside the MMI coupler. The range of refractive index is small enough for the tolerance of the MMI coupler, so the spatial hole-burning does not make some unstable operation, and the laser radiations of the mode-1 and mode-2 exist stably.

Conclusion

We have proposed and investigated a novel BLD with an active 2×2 MMI coupler. The static characteristics of the MMI-BLD have been simulated by using FD-BPM which takes into account the photon-carrier interaction through the carrier rate equation. We have predicted that the MMI-BLD shows bistable switching between the two cross-coupled modes by 0 dBm external light injection, which can be used as an all-optical flip-flop or an optical memory.

[1] G. J. Lasher, *Solid-State Electronics*, vol. 7, pp. 707-716, 1964.
[2] C. L. Tang, A. Schremer, and T. Fujita, *Appl. Phys. Lett.*, vol. 51, pp. 1392-1394, 1987.
[3] B. B. Jian, *Electron. Lett.*, vol. 32, no. 20, pp. 1923-1925, 1996.
[4] Y. Chung, and N. Dagli, *IEEE J. Quantum Electronics*, vol. 26, pp. 1335-1339, 1990.
[5] H. K. Bissessur, F. Koyama, and K. Iga, *IEEE J. Select. Topics in Quantum Electronics*, vol. 3, pp. 344-352, 1997.
[6] G. R. Hadley, *IEEE J. Quantum Electronics*, vol. 28, pp. 363-370, 1992.
[7] R. Olshansky, C. B. Su, J. Manning, and W. Powazinik, *IEEE J. Quantum Electronics*, vol. QE-20, pp. 838-854, 1984.
[8] M. Takenaka, and Y. Nakano, *COIN+PS2002*, PS.TuB5, pp. 78-80, Cheju Island, July, 2002.